Acta of Bioengineering and Biomechanics
Vol. 20, No. 1, 2018

Original paper
DOI: 10.5277/ABB-00969-2017-02

Assessment of corneal and fatty tissues biomechanical response in dynamic tonometry tests by using inverse models

MOHAMMAD JANNESARI[1], MAHMOUD KADKHODAEI[1], PEIMAN MOSADDEGH[1, 2], HENRYK KASPRZAK[3]*, MAHMOUD JABBARVAND BEHROUZ[4]

[1] Department of Mechanical Engineering, Isfahan University of Technology, Isfahan, Iran.
[2] Visiting Scholar, Computer Vision Laboratory, Institut für Bildverarbeitung, Department of Information Technology and Electrical Engineering, Swiss Federal Institute of Technology Zürich, Zürich, Switzerland.
[3] Faculty of Principal Problems of Technology, Wrocław University of Science and Technology, Wrocław, Poland.
[4] Eye Research Center, Farabi Eye Hospital, Tehran University of Medical Sciences, Tehran, Iran.

Purpose: The assessment of corneal biomechanics is essential for studying ophthalmological operations, such as refractive surgeries, and for more accurate estimation of intraocular pressure. The chief aim of the current study is to characterize corneal and fatty tissues in order to construct a model to predict eye globe behavior during dynamic tonometry tests. *Methods*: In the present study, images from corneal deformation, acquired from Corvis ST tonometer, were processed. Then, corneal pure displacement and eye globe retraction were calculated. Utilizing inverse finite element method, corneal material properties were calculated in order to predict pure deformation obtained from Corvis ST. Using a similar approach, material parameters of fatty tissue were estimated in order to predict the eye globe retraction. The model used for fatty tissue was considered as corneal boundary condition in a forward finite element model to create a joint model, which could simulate corneal behavior in dynamic tonometry tests. *Results*: It was shown that an isotropic material model is accurate enough to predict corneal deformation in dynamic tonometry tests. Moreover, effects of IOP on the estimated material properties were investigated. Finally, utilizing the joint model, it was demonstrated that there is strong correlation between corneal stiffness and the biomechanical parameter introduced by Corvis ST. *Conclusions*: An eye globe model was constructed and characterized by two distinct inverse models for corneal and fatty tissue. This model can be utilized for predicting eye globe behavior during dynamic tonometry tests besides other ophthalmological operations.

Key words: *corneal biomechanics, fatty tissue, dynamic tonometry, inverse finite element method*

1. Introduction

Cornea is a transparent tissue forming front of the eye and participating in refracting of the light on the retina. A healthy cornea generates about 70 percent of the total eye refractive power of about 60 diopters [15]. Consequently, variations in biomechanical and geometrical properties of cornea can intensely affect corneal refractive power and may interrupt the eye vision. Therefore, understanding of biomechanical behavior of cornea is a beneficial tool for recognizing cornea diseases, such as keratoconus [19]. Additionally, corneal biomechanical properties are essential for predicting cornea response in refractive surgeries [5] and for more accurate estimation of intraocular pressure [13].

Corneal material properties can be evaluated by several different *ex-vivo* and *in-vivo* methods. *Ex-vivo* investigations are accomplished on corneal strip [4], button inflation [7], and whole-globe inflation [3]. Surface wave propagation is an *in-vivo* method to quantitatively determine material properties of cornea. Elastic and viscoelastic properties of cornea tissue can be estimated using this method [6], [26]. Nonetheless, these investigations are carried out on *ex-vivo* samples, so the effectiveness of these methods in clinical applications has not been proven [18]. Applying the tonometers to measure intraocular pressure (IOP) is another *in-vivo* method to investigate cornea biome-

* Corresponding author: Henryk Kasprzak, Department of Optics and Photonics, Wrocław University of Science and Technology, 50-370 Wrocław, Poland. Phone: 0048 (71) 3203306, E-mail: Henryk.Kasprzak@pwr.edu.pl
Received: August 1st, 2017
Accepted for publication: October 17th, 2017

chanics. Tonometers are generally divided into two groups of contact tonometers, e.g., Goldmann tonometer, and non-contact ones, e.g., Ocular Response Analyser (ORA; Reichert, Inc.) and Corvis ST (CorVis ST; Oculus Optikgerate GmbH). In addition to IOP, some non-contact tonometers evaluate some biomechanical properties of cornea; for instance, ORA tonometer reports corneal hysteresis (CH) and corneal resistance factor (CRF) as corneal biomechanical properties. Corvis ST is another non-contact tonometer recently used for assessing biomechanical properties of cornea. Corvis ST tonometer applies a metered air puff in about 32 milliseconds with a maximum amplitude of 25 kPa [1]. Due to the applied pressure, cornea deforms; it passes through the first applanation and reaches the highest concavity configuration. Then, by reducing the amount of applied pressure, cornea begins to return to its natural shape by passing through the second applanation. This tonometer uses an ultra-high-speed camera capturing more than 4300 images per second to record cornea deformation during tonometry test. These images provide an efficient tool for assessing cornea biomechanical material properties. Recently, Corvis ST tonometer presented two novel stiffness parameters that can be used for screening corneas with keratoconus [25].

Luce studied the results of ORA tonometry test to estimate biomechanical properties of the cornea and their relationship to IOP [14]. He expressed that corneal hysteresis measured by ORA provides valuable data for qualification of refractive surgery outcomes. For instance, post-LASIK eyes showed low corneal hysteresis. Assessment of the biomechanical properties of cornea in normal and keratoconus eyes was conducted by Shah et al. [19]. Roy et al. estimated corneal elastic modulus after crosslinking by employing inverse finite element method [17]. In their study, patient-specific finite element models were constructed with the use corneal topography measured before crosslinking. Corneal properties were optimized using inverse optimization method in order to minimize differences between *in-vivo* corneal topography and theoretical prediction after crosslinking. A viscoelastic finite element model was presented by Kling et al. in order to predict *in-vivo* corneal deformation in various conditions [9]. Sensitivity analysis disclosed influence of IOP, corneal thickness, and corneal biomechanical properties on corneal deformation. Parametric study was accomplished by numerical model in order to estimate the effects of IOP and applied air jet pressure on mechanical behavior of cornea [21]. Cornea biomechanical behavior in non-contact tonometer was studied by considering an anisotropic hyperelastic material [2]. The influences of IOP, corneal thickness, and corneal stiffness on the apex displacement were investigated taking variation in the mentioned parameters into consideration. A patient-specific inverse finite element model was utilized in order to assess biomechanical properties of cornea from Corvis ST tonometry test [16]. The effectiveness of inverse finite element model in estimation of corneal material properties was shown in this study. Jannesari et al. (under review) determined appropriate material model for cornea by using images captured from Corvis ST. They quantitatively showed that the contribution of viscosity in cornea response in dynamic tonometry tests can be disregarded.

The main goal of the current study was an *in-vivo* assessment of on biomechanical properties of cornea and fatty tissue, based on images captured from Corvis ST tonometer. Cornea deformations were determined using profiles obtained with the use of image processing techniques. Cornea pure deformation and eye globe movement are decoupled from corneal profiles. Employing inverse finite element method (FEM), which is a combination of FEM and an optimization algorithm, corneal biomechanical properties were then evaluated in order to obtain corneal pure deformation. Similarly, biomechanical properties of fatty tissue were determined using the combination an ODE solver and an optimization algorithm in order to reach eye globe movement. The influence of IOP on the estimated corneal material properties was also studied in present paper. Finally, influences of test parameters on the corneal biomechanical parameters reported by ORA and Corvis ST tonometers were investigated by the current approach.

2. Materials and methods

Deformation of cornea is influenced by its biomechanical properties and resistance of the fatty tissue. In this work, cornea deformation of five healthy eyes was obtained from images captured from Corvis ST tonometer by using image processing techniques introduced by Koprowski et al. [11], [12]. The deformation curves acquired from Corvis ST tonometer were decoupled and converted to eye globe rigid body movement (retraction) and corneal pure deformation. Corneal pure deformation shows cornea indentation due to the applied air puff in Corvis ST tonometry test. It describes displacement of 576 equally-spaced points on anterior surface of cornea over 140 instances in which Corvis ST captures images from corneal deformation. In addition to fatty tissue located behind the

eye globe, there are six muscles responsible for its movement. These tissues affect the eye globe deformation when a force, i.e., air pressure, is applied on the corneal surface. Due to flexibility of the fat tissue, eye globe can move backward when a force is applied on the anterior eye. Indeed, retraction depicts eye globe movement toward fatty tissue located behind the eye and also shows deformation of the fatty tissue (Jannesari et al., under review). As a typical response, total and pure displacements of the apex together with eye globe retraction are all shown for a healthy eye in Fig. 1.

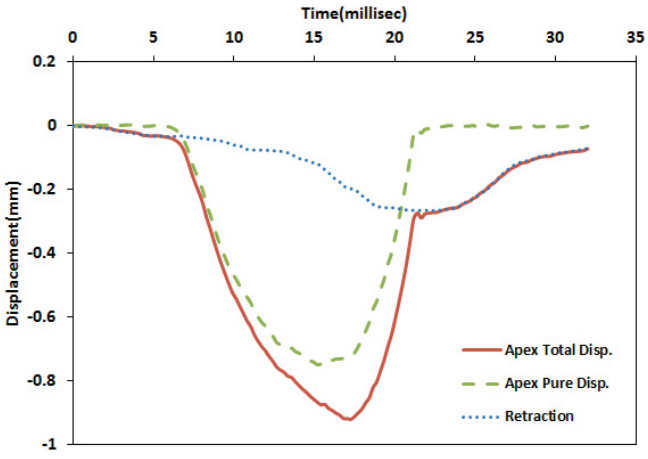

Fig. 1. Variations of total and pure displacement of apex point as well as the whole eye globe retraction for a healthy eye in time (Jannesari et al., under review)

In the present study, corneal material properties are estimated in order to reach corneal pure deformation obtained from Corvis ST by utilizing inverse finite element model. Similarly, assuming a simple one-dimensional model for fatty tissue, material constants of the selected model are estimated in order to reach eye globe retraction.

2.1. Determination of corneal material properties

In this subsection, the inverse finite element model utilized for characterization of the cornea tissue is described. Inverse finite element model is a mixture of an optimization method and a finite element model. Levenberg–Marquardt least square algorithm, as an optimization approach, is employed to estimate material properties of the cornea. According to the flowchart shown in Fig. 2, the guesstimated material properties are passed to finite element solver, i.e., Abaqus FE release 6.14. Then, Corvis ST tonometry test is run using the finite element model considering the estimated material properties. Afterwards, the corneal deformation obtained from the finite element model is returned to the optimization algorithm. Levenberg–Marquardt algorithm compares finite element solution with corneal pure deformation obtained from Corvis ST and is set to reduce their differences by modifying the estimated material properties. The optimization process continues until the finite element solution converges to pure cornea deformation obtained from Corvis ST by considering a reasonable error tolerance.

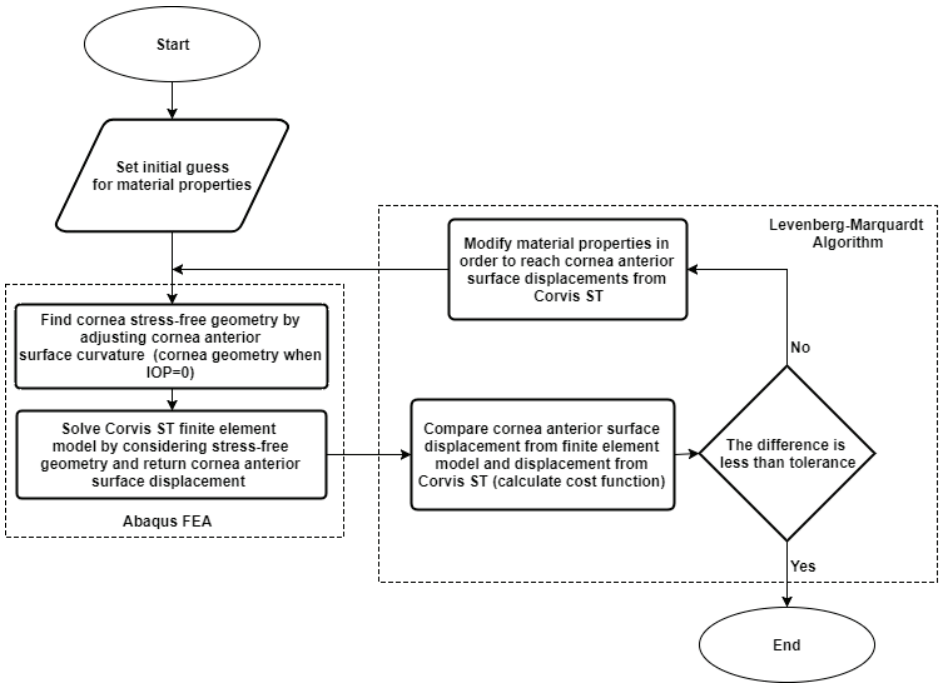

Fig. 2. Inverse finite element model to determine corneal material properties

2.1.1. Finite element model

Corvis ST tonometry test was simulated in a finite element model by considering estimated material properties in order to calculate corneal surface deformation. In the following subsections, different aspects of finite element model such as the model geometry, material model, boundary conditions, and loading conditions are described.

Corneal Geometry

Cornea is considered as a two-dimensional axisymmetric geometry in Abaqus CAE. The geometry of cornea was obtained from the first image captured from Corvis ST which shows the cornea in its undeformed configuration. Using the image processing techniques introduced by Koprowski et al. [11], [12], coordinates of 576 points on the anterior surface and 576 on the posterior surface of cornea were obtained. All the points were imported into Abaqus CAE 6.14 and connected to each other via splines. This process was accomplished for each case separately. Figure 3 shows corneal axisymmetric geometry for a healthy eye which is modeled in Abaqus CAE.

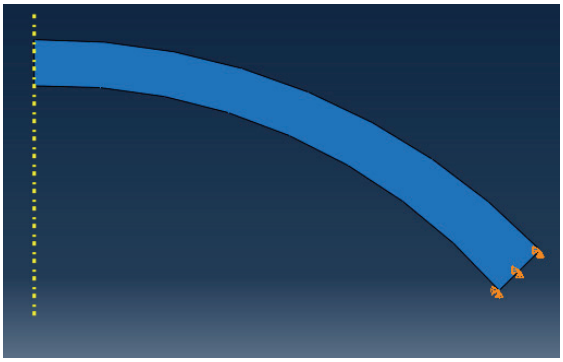

Fig. 3. Cornea as a two-dimensional axisymmetric geometry; yellow dotted line shows the axis of symmetry

Cornea material model

Appropriate cornea material model in the simulation of non-contact tonometry tests has been a controversial issue in biomechanics. Su et al. Proposed a hyper-viscoelastic material model for considering both elasticity and viscosity of cornea [24]. The material parameters of their model were characterized by using uniaxial tensile tests and stress relaxation experiments. Kling et al. considered cornea as a viscoelastic material and calculated material properties from *in-vivo* air puff deformation [9]. Conversely, due to high loading rate in Corvis ST tonometry test, cornea was assumed to behave as a hyperelastic material by Roy et al. [21]. Simonini et al. qualitatively showed that cornea behavior in Corvis ST tonometry test is not affected by viscosity of the material [20]. Comparing corneal retardation time and air puff loading interval, Jannesari el al. (under review) expressly showed that cornea behaves as a hyperelastic material in non-contact tonometry tests. Therefore, a hyperelastic material model must be chosen for cornea material model. Although cornea is intrinsically anisotropic, isotropic material models can also predict corneal behavior with enough accuracy. Moreover, it is obvious that the number of material constants affects uniqueness of the estimated material properties. The bigger the number of material model constants, the more flexible the inverse finite element model and probably the less unique the estimated material properties. Since all studies presented will be conducted with the same loading regime (applied air puff), it is not necessary to choose anisotropic material model. Indeed, selecting anisotropic material model increases flexibility of the model and causes non-uniqueness issues. However, the material model must be flexible enough to simulate cornea deformation in Corvis ST tonometry test. Consequently, Neo-Hookean hyperelastic material model is an appropriate choice for satisfying both uniqueness and flexibility.

The constitutive equation of Neo-Hookean hyperelastic material model is defined as [23]

$$\sigma = \frac{2C_{10}}{J}\,\mathrm{dev}(J^{-\frac{2}{3}}\boldsymbol{F}\boldsymbol{F}^{\boldsymbol{T}}) + 2D_1(J-1)\boldsymbol{I}, \qquad (1)$$

in which C_{10} and D_1 are model constants, $\boldsymbol{F}$ is deformation gradient tensor, $\boldsymbol{J}$ is determinant of deformation gradient tensor, and $\boldsymbol{I}$ is identity tensor. The deviatoric part of a tensor is shown by dev(*) operator. Since cornea is almost incompressible [22], an additional constraint must be considered. Equation 2 defines a relation between material properties and Poisson ratio, which must be greater than 0.45 in order for the material to be almost incompressible.

$$\nu = \frac{3 - 2C_{10}D_1}{6 + 2C_{10}D_1} > 0.45. \qquad (2)$$

Boundary conditions and loads

Since corneal pure deformation from the model is compared with the one obtained from Corvis ST, the cornea is supposed to be completely fixed at limbus (its boundary). IOP is applied at the posterior surface of cornea as a constant uniform pressure. Air puff applied on the anterior surface of cornea is also considered as a variable pressure with time and position, as reported by Ariza-Gracia et al. [2].

Load steps

In the first loading step, IOP is applied on the posterior surface of the cornea. The initial corneal geometry obtained from Corivs ST tonometer is a stressed configuration, and it would differ from the obtained geometry after applying IOP. Consequently, in the first step of analysis, a pre-initial geometry is calculated for the cornea. This geometry reaches the initial geometry after applying IOP. Air puff is applied on the anterior surface of cornea in the second step of analysis. The first step needs a static analysis while the second one is a dynamic case.

2.1.2. Optimization algorithm

In order to minimize differences between the corneal deformation obtained from finite element model and the one obtained from Corvis ST, Levenberg–Marquardt least square algorithm is employed. The objective function to be minimized is formulated as,

$$\chi^2 = \sum_{i=1}^{m}\left(\sum_{j=1}^{p}[u_{CST}(t_i, r_j) - u_{FE}(t_i, r_j; x)]\right)^2, \quad (3)$$

in which u_{CST} is displacement of corneal anterior surface from Corvis ST, u_{FE} – displacement of corneal anterior surface from the finite element model, t_i – measurement time, r_j – distance from corneal apex, m and p – number of instances and points at which the objective function is calculated, $x = [C_{10}, D_1]$ vector of material properties, and χ – the objective function that shows error tolerance. The optimization algorithm was implemented in Matlab through a home-made code and was linked to Abaqus FE solver via a home-made python library. As the optimization algorithm may yield local minima, the optimization process was repeated with different initial guesses to make sure about finding global minimum. Moreover, the optimization algorithm needs the Jacobian test of the cost function which is evaluated numerically.

2.2. Fat tissue characterization

In order to make the corneal model more accurate, it is necessary to consider the effects of fatty tissue on the eye globe deformation. These effects will be considered in the corneal model as boundary conditions. It was shown that the fatty tissue shows viscoelastic response during dynamic tonometry tests (Jannesari et al.; under review). Therefore, as can be seen in Fig. 4, a parallel combination of spring and dashpot series with a lumped mass, showing the eye globe mass, is considered for modeling the fatty tissue for the sake of simplicity.

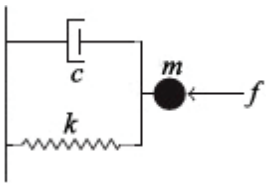

Fig. 4. Fat tissue model: a parallel combination of spring and dashpot which is series with a lumped mass

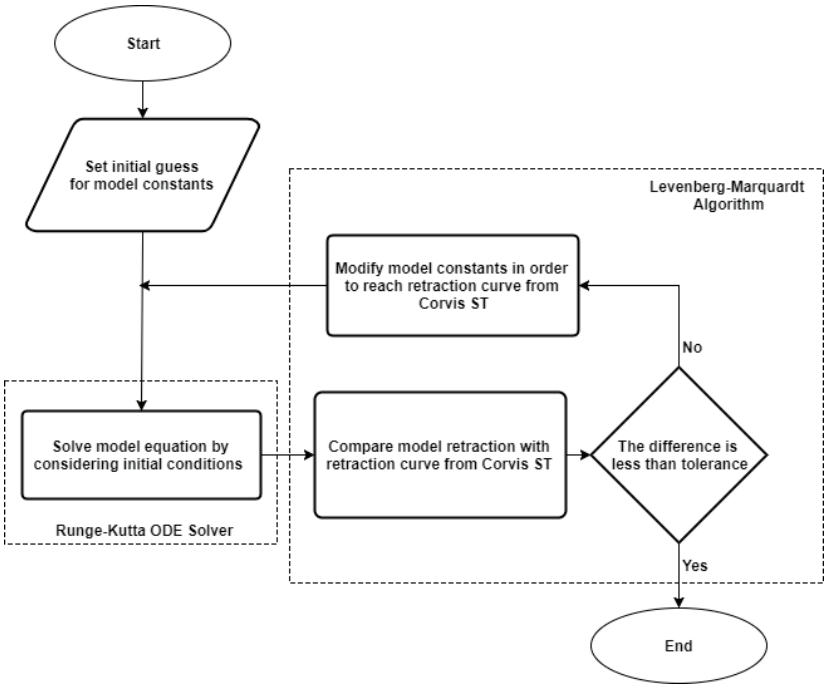

Fig. 5. Characterizing process utilized for calculating fatty tissue model constants

The governing equation for the fatty tissue model is formulated as,

$$m\ddot{z} + c\dot{z} + kz = f, \tag{4}$$

in which m, c, and k are model constants, z – eye globe displacement, and f – applied force to the fatty tissue due to the applied air puff, which is obtained from the corneal finite element model. A similar process to the one accomplished for characterizing the cornea is employed for estimating constants in the fatty tissue model. The optimization algorithm approximates the model parameters to minimize the objective function, defined as,

$$\chi^2 = \sum_{i=1}^{140} [z(t_i)_{\text{Model}} - z(t_i)_{CST}]^2, \tag{5}$$

where $z(t_i)_{\text{Model}}$ is displacement at instance t_i calculated from the model, and $z(t_i)_{CST}$ is the one obtained from Corvis ST tonometry. The objective function, χ, is summed over 140 instances between 0 to 32 milliseconds during which images were exported. Figure 5 shows flowchart of the implemented algorithm in details. Displacement obtained from the model, $z(t_i)_{\text{Model}}$, is calculated by solving Eq. (4) with Runge–Kutta ODE solver coupled with Levenberg–Marquardt least square algorithm. To make sure of finding the global minimum, the optimization process was started with different initial guesses.

2.3. Combination of corneal and fat tissue models

After determining the material properties of both models, they are coupled with each other in a forward finite element model, as shown in Fig. 6. The fatty tissue model is coupled with the corneal forward finite element model as the boundary condition at Limbus.

This model, which almost represents behavior of the eye globe in tonometry tests, is used to assess corneal biomechanical properties provided by ORA and Corvis ST. ORA reports corneal resistance factor (CRF) and corneal hysteresis (CH) as the corneal biomechanical properties. Recently, Corvis ST introduced SP-A1 and SP-HC as two novel stiffness parameters to be strong indicators of corneal biomechanical properties [25]. SP-A1 is calculated by dividing the resultant pressure on the cornea by corneal displacement from undeformed configuration to the first applanation.

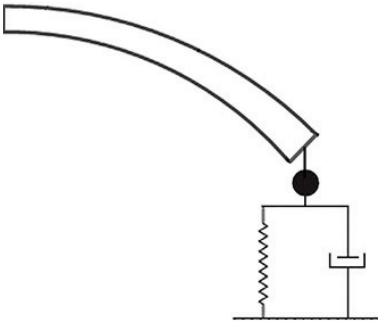

Fig. 6. Forward joint model for imposing corneal behavior in IOP measurement process

3. Results

Corneal and fatty tissue's biomechanical properties calculated by the optimization processes are presented within two distinct subsections. Additionally, reliability of the corneal biomechanical parameters measured by ORA and Corvis ST tonometers is assessed by using the joint model in the last part.

3.1. Cornea characterization

Since an inverse problem may cause non-unique solutions due to ill-poseness, the ill- or well-poseness of the problem must be initially assessed. Hence, three different virtual corneal displacements are created using forward finite element model by assuming three different sets of the material properties. Then, the inverse model tries to find the assumed material properties for each of these three virtual displacements. Moreover, to study the robustness of the inverse model, virtual displacements were polluted with Gaussian noise and virtual tests were repeated. Details of the virtual tests are brought in Table 1.

Table 1. Results of the virtual tests to make sure about well-poseness of the inverse problem

Assumed material properties		Initial guesses		χ^2 [$10^{-3} \times$ mm^2]	
C_{10} [kPa]	D_1 [$10^{-6} \times$ kPa^{-1}]	C_{10} [kPa]	D_1 [$10^{-6} \times$ kPa^{-1}]	Noiseless	Noisy
100	150	300	50	1.52	2.13
250	300	100	100	1.21	1.84
350	250	500	150	1.08	1.97

As shown in Table 1, the inverse model for characterizing cornea is well-posed and robust to noise. So, the material properties calculated by the model are credible.

After making certain whether the inverse model is a correct choice, five healthy cases in the age range of 25 to 30 years old were studied. Clinical data were gathered in accordance with the principles of the Declaration of Helsinki. All data gathered were analyzed and pure deformation of cornea and eye globe retraction were obtained. The corneal material properties were obtained for 3 different amounts of IOP based on corneal pure deformation and listed in Table 2.

Table 2. Calculated material properties for 5 heathy cases in 3 different IOP reports as mean ± standard deviation

IOP [mmHg]	C_{10} [kPa]	D_1 [$10^{-6} \times$ kPa^{-1}]	χ^2 [mm^2]
12	336 ± 27	182 ± 1	0.097 ± 0.013
16	316 ± 27	185 ± 1	0.089 ± 0.020
20	294 ± 28	185 ± 1	0.094 ± 0.006

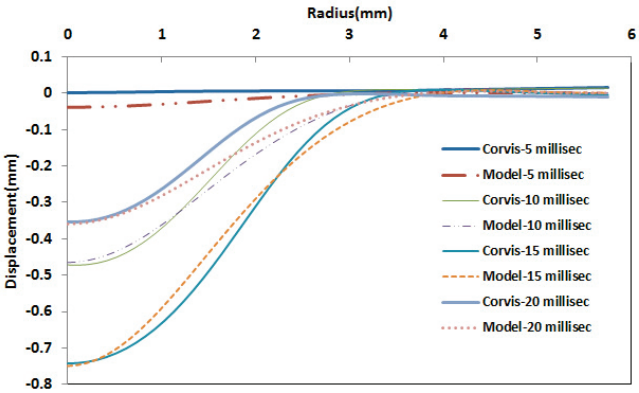

Fig. 7. Variation of corneal surface displacement with radius of cornea at four different instances for the first case

Displacements of the corneal surface at four instances are shown in Fig. 7. It can be seen that deformation obtained from the model is in a good agreement with the experimental results. Figure 8 shows time variation of corneal apex point in three different amounts of IOP for the first case. This figure shows that corneal behavior in time can be also predicted by the model.

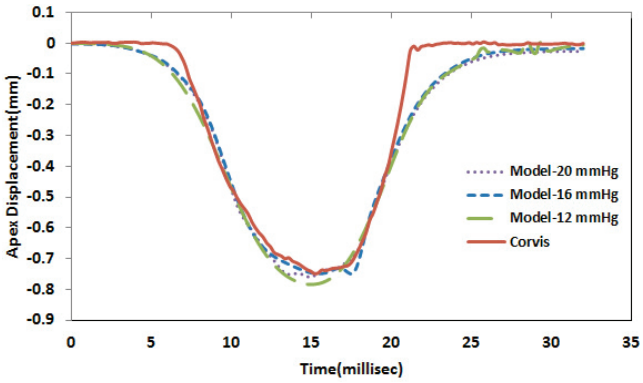

Fig. 8. Comparison of time variation of apex displacement between model and Corvis ST at three different amounts of IOP

Although the model considered for the cornea is an isotropic model with the minimum number of material properties, the model enables prediction of the corneal behavior with reasonable accuracy in different evaluated times and positions. The errors observed may be caused by different reasons, such as inaccuracy in spatial or temporal air puff distribution and simplicity of the assigned material model.

3.2. Fat tissue characterization

The ill- or well-poseness of the inverse model for characterizing the fatty tissue must be initially assessed, similarly to what was done for characterizing the corneal tissue. By considering three sets of virtual material constants for the fatty tissue, Eq. (4) was solved and the virtual eye globe retraction was calculated for each set. Subsequently, the inverse model for

Table 3. Results of the virtual tests for assessment of well-poseness in the fatty tissue inverse model

Assumed material properties			Initial guesses			χ^2 [mm^2]	
k [N/m]	c [N sec/m]	m [g]	k [N/m]	c [N sec/m]	m [g]	Noiseless	Noisy
500	1	5	200	3	10	6.76×10^{-31}	1.96×10^{-2}
150	2.5	12	300	7	3	1.96×10^{-31}	1.96×10^{-2}
300	2	7	420	15	15	6.15×10^{-31}	1.86×10^{-2}

Table 4. Obtained material constants for the fatty tissue model as mean ± standard deviation for five healthy cases

k [N/m]	c [N sec/m]	m [g]	χ^2 [mm^2]
592.96 ± 106.43	2.60 ± 0.23	10.64 ± 3.14	$5.28 \times 10^{-2} \pm 3.82 \times 10^{-3}$

the fatty tissue endeavored to find the material constants for each virtual retraction. The results of virtual tests, for both noisy and noiseless virtual retractions, are provided in Table 3.

Since the inverse model for characterization of the fatty tissue is successful in determination of assumed material constants for both virtual reactions, it can be considered as a well-posed and robust model. After approving the inverse model, by considering the eye globe retractions of five healthy cases, the material constants of the fatty tissue model are calculated as listed in Table 4. Time variation of the retraction for the first case, which is depicted in Fig. 9, shows the ability of the model to simulate eye globe retraction nevertheless the model is a simple one-dimensional rheological one.

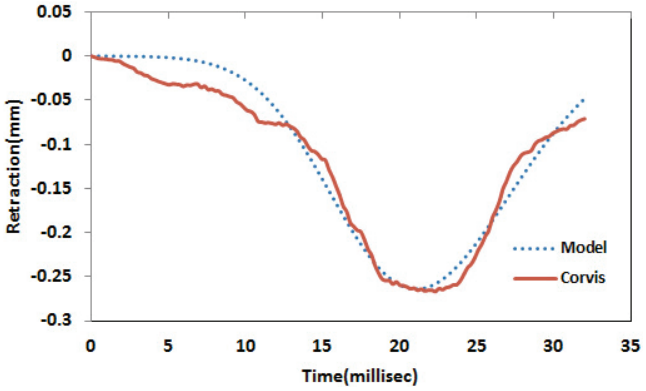

Fig. 9. Variation of eye globe retraction for the first case, comparison between model and Corvis ST

3.3. Joint model

To assess accuracy of the separate modeling, i.e., decoupling of the eye globe retraction and corneal pure deformation, the joint model is stimulated by using Corvis ST applied air puff so that the corneal total deformation is obtained. In Figure 10 variations of the apex total displacement with time received from both Corvis ST experimental data and the joint finite element model are shown.

To assess the biomechanical parameters reported by tonometers, CH and SP-A1 are obtained from the joint model and brought in Table 5 for different values of IOP. These quantities are two corneal biomechanical parameters which are respectively reported by ORA and Corvis ST tonometers. Additionally, variation of these two parameters with maximum applied pressure is brought in Table 6. Figure 11 shows correlation between parameters SP-A1 and C_{10} in the Neo-Hookean material model.

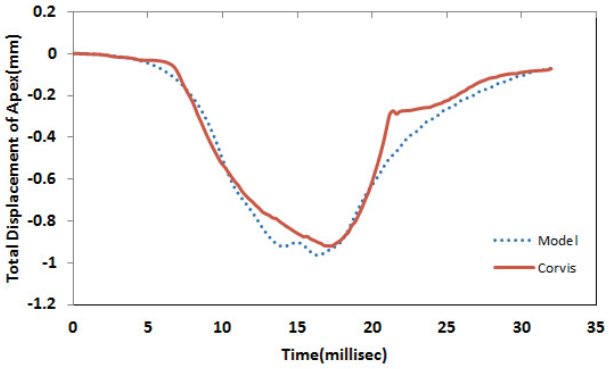

Fig. 10. Comparison between total displacements from the joint model and Corvis ST for assuring about decoupling assumption

Table 5. Corneal hysteresis and SP-A1 for different values of IOP when all material properties are kept constant and maximum air puff pressure is 25 kPa

IOP [mmHg]	CH [kPa]	SP-A1 [kPa/mm]
12	1.50	22.08
14	1.45	22.08
16	0.90	22.15
18	0.45	22.16
20	0.30	21.31
22	0.95	21.90
24	0.95	21.78
Mean	0.93	21.92
Standard Deviation	0.45	0.31

Table 6. Effect of maximum applied pressure on corneal hysteresis and SP-A1 when all material properties are remained constant and IOP is 16 mmHg

Air puff [kPa]	CH [kPa]	SP-A1 [kPa/mm]
20	1.80	21.92
30	0. 31	22.09
40	0. 41	21.81
50	0.44	22.33
Mean	0.74	22.04
Standard Deviation	0.71	0.22

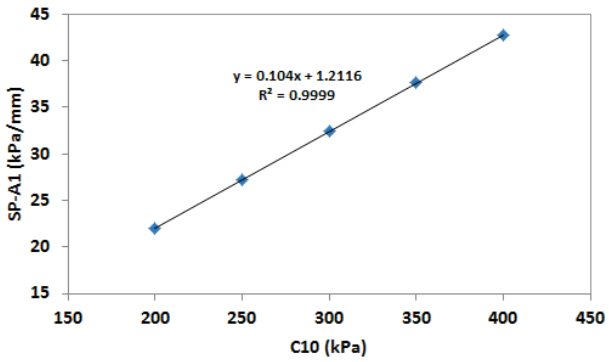

Fig. 11. Correlation between parameter C_{10} and SP-A1 in the joint model where IOP = 16 mmHg, D_1 = 185 kPa, and maximum air puff pressure is 25 kPa

4. Discussion

Different studies were conducted on the *in vivo* assessment of corneal biomechanical properties [9], [21]. Some of them ignore the effects of eye globe boundary conditions, which result from the existence of fatty tissue and muscles. Roy et al. suggested the use a parallel combination of spring and dashpot series with a lumped mass for considering the effects of boundary conditions [16]. The material constants for the corneal model and those for the fatty tissue were all calculated by one optimization process. In the current study, corneal and fatty tissue properties were individually calculated by decoupling corneal pure deformation and eye globe retraction. Individual optimization processes for the cornea and the fatty tissue increase the well-poseness of inverse algorithm and yield more reliable material properties.

Most of the studies on corneal characterization have selected anisotropic fibril-dependent hyperelastic material model. However, the corneal displacement from both model and Corvis ST depicted in Fig. 7 shows that the presented isotropic material model in this work is accurate enough to model corneal behavior. As mentioned before, anisotropic material models must be used when the loading type changes between characterization process and further investigations. Additionally, selection of anisotropic material model increases the number of unknown material properties and requires extra experiments with different loading regimes to obtain reliable material properties [10]. Nonetheless, application of an anisotropic model may decrease errors between model predictions and Corvis ST results. The findings listed in Table 3 show that cornea with higher IOP is more compliant [21]. Indeed, the higher value of IOP yields more resistant force against corneal deformation, so the cornea must be more compliant to deform enough. The variation of corneal material properties in different amounts of IOP is about 10 percent, and it mostly affects C_{10}. The coefficients C_{10} and D_1, respectively, describe rigidity and compressibility of the cornea. Consequently, change in the amount of IOP only makes C_{10} to vary and does not considerably affect compressibility of the tissue. The mass of the eye globe, which is denoted by parameter m in Table 4, is nearly equal to the experimentally-measured number [8]. This confirms that the obtained material constants are reliable. In other words, calculation of the material properties in one optimization process may lead to non-physical values for the obtained material parameters.

An important assumption, considered in the proposed separate modeling, is independence of corneal deformation and eye globe retraction. Indeed, it was assumed that these two deformations have no effects on each other for the modeling purposes. As can be seen in Fig. 10, good agreement between the obtained results from model and experiments show that this assumption is reasonable. This means that the joint model truly predicts the corneal behavior during Corvis ST tonometry test. It should be mentioned that effects of the sclera and other components of the eye are disregarded in this model due to lack of reliable data in the literature.

As listed in Tables 5 and 6, corneal hysteresis varies with changes in IOP and the maximum applied pressure while SP-A1 is almost constant. This shows that corneal hysteresis cannot be related to biomechanical properties of cornea. This issue was also mentioned by Simonini and Pandolfi who related the corneal hysteresis to dynamics of the corneal elastic structure in their studies [21]. In direct contrast to corneal hysteresis, SP-A1 is almost constant during variations of IOP and applied pressure; this means independency of this parameter from test conditions. Moreover, as seen in Fig. 11, SP-A1 shows strong correlation with material model parameter C_{10}. These all show strong correlation between corneal biomechanical properties and the parameter SP-A1.

5. Conclusion

In the present study, material properties of cornea and fatty tissue were calculated by using separate optimization processes. Although the proposed isotropic material model simulates corneal deformation with enough accuracy, fibril-dependent anisotropic hyperelastic material can be utilized to increase quality of the model. In this manner, 3-D geometry must be considered for the cornea since the fibril distribution in the cornea is not axisymmetric. It should be noticed that Corvis ST captures corneal deformation at a fixed horizontal imaging plane, so 3-D deformation of cornea cannot be acquired from such images. Accordingly, it seems that modeling cornea as an isotropic axisymmetric body is an appropriate choice for characterizing cornea by using data from Corvis ST tonometer. The greatest advantage of this study is different optimization processes that give information about the cornea and the fatty tissue separately. Corneal deformation was tracked during the time, and time-dependent deformations of corneal and fatty tissue were considered for optimization. It was shown that the

parameter SP-A1 introduced by Corvis ST truly expresses a biomechanical property of the cornea whereas corneal hysteresis parameter presented by ORA varies according to changes in non-biomechanical parameters.

Acknowledgements

The authors thank Reza Ghaffari, MD (Farabi hospital, Tehran, Iran), Soheila Asgari, MD (Ophthalmology Research Center, Noor Eye Hospital, Tehran, Iran), and Hesam Hashemian, MD (Farabi hospital, Tehran, Iran) for assistance with collecting Corivs ST data from Noor Ophthalmology Research Center, Noor Eye Hospital, Tehran, Iran. Ali R Djalilian, MD (Department of Ophthalmology and Visual Sciences, University of Illinois at Chicago, IL) is acknowledged for his generosity and valuable comments on the current research.

References

[1] AMBRYSIO JR R., RAMOS I., LUZ A., FARIA F.C., STEINMUELLER A., KRUG M., BELIN M.W., ROBERTS C.J., *Dynamic ultra high speed Scheimpflug imaging for assessing corneal biomechanical properties*, Rev. Bras. Oftalmol., 2013, 72(2), DOI: 10.1590/s0034-72802013000200005.

[2] ARIZA-GRACIA M.Б., ZURITA J.F., PICERO D.P., RODRIGUEZ--MATAS J.F., CALVO B., *Coupled Biomechanical Response of the Cornea Assessed by Non-Contact Tonometry. A Simulation Study*, PLOS ONE, 2015, 10(3), DOI: 10.1371/journal.pone.0121486.

[3] ASEJCZYK-WIDLICKA M., PIERSCIONEK B., *The elasticity and rigidity of the outer coats of the eye*, Br. J. Ophthalmol., 2008, 92(10), DOI: 10.1136/bjo.2008.140178.

[4] BOYCE B., JONES R., NGUYEN T., GRAZIER J., *Stress-controlled viscoelastic tensile response of bovine cornea*, J. Biomech., 2007, 40(11), DOI: 10.1016/j.jbiomech.2006.12.001.

[5] BRYANT M.R., MCDONNELL P.J., *Constitutive laws for biomechanical modeling of refractive surgery*, J. Biomech. Eng., 1996, 118(4), DOI: 10.1115/1.2796033.

[6] DUPPS W.J., NETTO M.V., HEREKAR S., *Surface wave elastometry of the cornea in porcine and human donor eyes*, J. Refract. Surg., 2007, 23(1).

[7] ELSHEIKH A., ANDERSON K., *Comparative study of corneal strip extensometry and inflation tests*, J. R. Soc. Interface, 2005, 2(3), DOI: 10.1098/rsif.2005.0034.

[8] KAMPMEIER J., RADT B., BIRNGRUBER R., BRINKMANN R., *Thermal and biomechanical parameters of porcine cornea*, Cornea, 2000, 19(3), DOI: 10.1097/00003226-200005000-00020.

[9] KLING S., BEKESI N., DORRONSORO C., PASCUAL D., MARCOS S., *Corneal Viscoelastic Properties from Finite-Element Analysis of In Vivo Air-Puff Deformation*, PLoS ONE, 2014, 9(8), DOI: 10.1371/journal.pone.0104904.

[10] KOK S., BOTHA N., INGLIS H.M., *Calibrating corneal material model parameters using only inflation data: An ill-posed problem*, Int. J. Numer. Method Biomed. Eng., 2014, 30(12), DOI: 10.1002/cnm.2667.

[11] KOPROWSKI R., KASPRZAK H., WRÓBEL Z., *New automatic method for analysis and correction of image data from the Corvis tonometer*, Comput. Methods Biomech. Biomed. Eng. Imaging Vis., 2014, DOI: 10.1080/21681163.2014.959137.

[12] KOPROWSKI R., LYSSEK-BORON A., NOWINSKA A., WYLEGALA E., KASPRZAK H., WROBEL Z., *Selected parameters of the corneal deformation in the Corvis tonometer*, Biomed. Eng. Online, 2014, 13(1), DOI: 10.1186/1475-925X-13-55.

[13] LIU J., ROBERTS C.J., *Influence of corneal biomechanical properties on intraocular pressure measurement: quantitative analysis*, J. Cataract Refract. Surg., 2005, 31(1).

[14] LUCE D.A., *Determining in vivo biomechanical properties of the cornea with an ocular response analyzer*, J. Cataract Refract. Surg., 2005, 31(1), DOI: 10.1016/j.jcrs.2004.10.044.

[15] PICERO D.P., ALCYN N., *In vivo characterization of corneal biomechanics*, J. Cataract Refract. Surg., 2014, 40(6), DOI: 10.1016/j.jcrs.2014.03.021.

[16] ROY A.S., KURIAN M., MATALIA H., SHETTY R., *Air-puff associated quantification of non-linear biomechanical properties of the human cornea in vivo*, J. Mech. Behav. Biomed. Mater., 2015, 48, DOI: 10.1016/j.jmbbm.2015.04.010.

[17] ROY A.S., ROCHA K.M., RANDLEMAN J.B., STULTING R.D., DUPPSAD W.J., *Inverse computational analysis of in vivo corneal elastic modulus change after collagen crosslinking for keratoconus*, Exp. Eye Res., 2013, 113, DOI: 10.1016/j.exer.2013.04.010.

[18] RUBERTI J.W., SINHA ROY A., ROBERTS C.J., *Corneal biomechanics and biomaterials*, Annu. Rev. Biomed. Eng., 2011, 13, DOI: 10.1146/annurev-bioeng-070909-105243.

[19] SHAH S., LAIQUZZAMAN M., BHOJWANI R., MANTRY S., CUNLIFFE I., *Assessment of the biomechanical properties of the cornea with the ocular response analyzer in normal and keratoconic eyes*, Invest. Ophthalmol. Vis. Sci., 2007, 48(7), DOI: 10.1167/iovs.04-0694.

[20] SIMONINI I., ANGELILLO M., PANDOLFI A., *Theoretical and numerical analysis of the corneal air puff test*, J. Mech. Phys. Solids, 2016, 93, DOI: 10.1016/j.jmps.2016.04.012.

[21] SIMONINI I., PANDOLFI A., *The influence of intraocular pressure and air jet pressure on corneal contactless tonometry tests*, J. Mech. Behav. Biomed. Mater., 2015, DOI: 10.1016/j.jmbbm.2015.07.030.

[22] SIMONINI I., PANDOLFI A., *Customized finite element modelling of the human cornea*, PLOS ONE, 2015, 10(6), DOI: 10.1371/journal.pone.0130426.

[23] DE SOUZA NETO E.A., PERIC D., OWEN D.R., *Computational methods for plasticity: theory and applications*, John Wiley & Sons, 2011.

[24] SU P., YANG Y., XIAO J., SONG Y., *Corneal hyper-viscoelastic model: derivations, experiments, and simulations*, Acta Bioeng. Biomech., 2015, 17(2), DOI: 10.5277/ABB-00142-2014-03.

[25] VINCIGUERRA R., AMBRYSIO R., ELSHEIKH A., ROBERTS C.J., LOPES B., MORENGHI E., AZZOLINI C., VINCIGUERRA P., *Detection of Keratoconus With a New Biomechanical Index*, J. Refract. Surg., 2016, 32(12), DOI: 10.3928/1081597x-20160629-01.

[26] ZHANG X., YIN Y., GUO Y., FAN N., LIN H., LIU F., DIAO X., DONG C., CHEN X. et al., *Measurement of quantitative viscoelasticity of bovine corneas based on lamb wave dispersion properties*, Ultrasound Med. Biol., 2015, 41(5), DOI: 10.1016/j.ultrasmedbio.2014.12.017.